

PM BLDC Motor with Toroidal Windings

Joachim Näf, Aramis Ringgenberg¹

1 Introduction

In this article we describe a permanent magnet brushless DC motor with toroidal windings and three phases. The use of toroidal windings in electrical machines has been suggested several times, as shown by the patents US4087711, US4373148, US4547713, US5175462, US5977684, US6700271, US20070228860A1 and US20140125155A1, e.g.. Independently of this, we discovered this possibility while searching for suitable motor geometries. Due to the simple design and our measurement results, we consider it desirable to promote the use of toroidal windings in motor construction.

There are some similarities, but also significant differences between the machines described in the above patents and the RNT motor² presented here. For example, the motor described in US5977684 shows some parallels both in terms of its construction and its functional principle. However, a ferromagnetic winding core is used there, and in addition, the staggered winding of the three phases with complete toroidal coils, which is typical for the RNT motor, is not required. This staggered winding is however found in US4373148. The motor described there is a brushless permanent magnet inrunner motor with four toroidal coils and two phases. The RNT motor, on the other hand, has three toroidal coils, each of which is assigned to a different phase.

In particular, the RNT motor has the following features:

- The motor is electronically commutated (EC) and requires a suitable control system for operation. Depending on the controller, sensors are required to determine the position of the rotor.
- The motor has a high starting torque, and since the winding core is made of a non-ferromagnetic material, both cogging torque and hysteresis loss are eliminated. The motor thus combines the positive characteristics of EC motors and induction motors.
- With appropriate scaling, the motor provides sufficient torque to drive at least smaller vehicles such as electric bicycles, motorcycles or compact cars without a mechanical gearbox. An upscaling of the motor concept for higher power and thus the gearless propulsion of larger vehicles is also conceivable, but has not been implemented by us so far. However, propulsion without a mechanical gearbox requires higher currents, and the efficiency is rather low at low RPM and high load. If necessary, propulsion can also be carried out using an axle gear.
- Depending on the proportions and volume of the winding core, liquid cooling inside the coils is possible.
- Depending on the design, the motor has an efficiency of more than 90% in various power classes and over a wide operating range.
- Like most electric motors, the RNT motor can also be used as a generator. However, we have not yet carried out any systematic measurements with our prototypes.
- The motor has a simple construction and can even be handcrafted in a suitably equipped workshop.

¹info@r-n-t.ch

²The abbreviation “RNT” refers to “Ringgenberg-Näf-Toroid”.

In this documentation we do not claim to present a formally proper scientific article. Rather, it is intended to explain the basic structure and the functional principle. The figures are for illustration purposes and are intended to contribute to understanding, but do not fulfil any standard for technical drawings.

2 Basic Design

Figure 1 shows the basic design of the RNT motor schematically. The illustration is exemplary and shows only one of many possible variations.

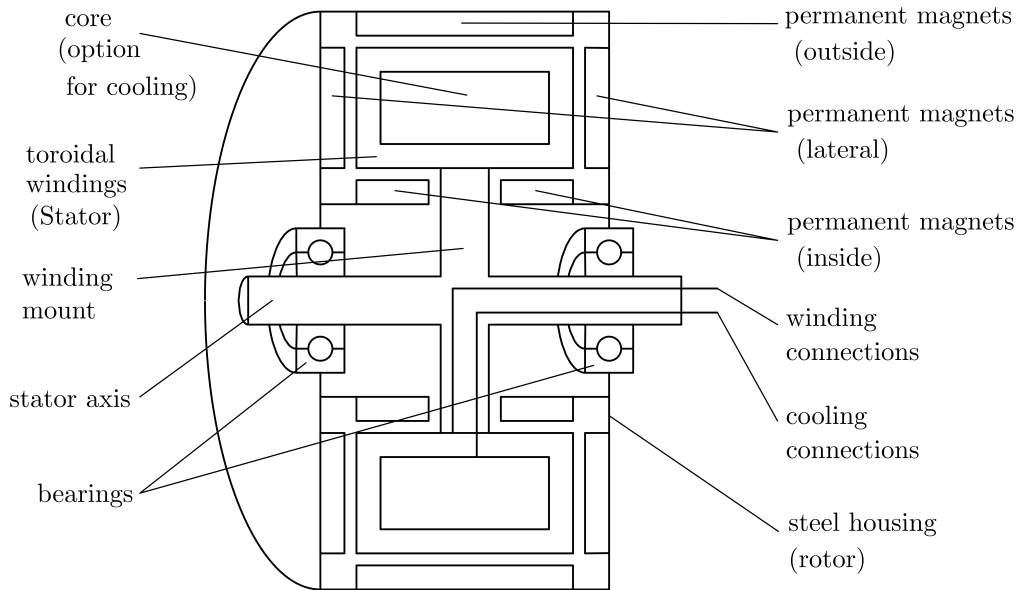


Fig. 1: Schematic representation of an RNT motor (for the sake of clarity, we have omitted a perspective view of the motor interior). The magnets can be mounted inside and outside as well as laterally of the stator. The connections for the windings and cooling are routed along or inside the winding mount to the stator axis. From there the connections are routed inside the axis.

The most important variations in the basic construction include:

- **Rotor:**

Depending on whether magnets are mounted inside, outside or laterally of the stator, the motor can in principle be designed as an inrunner, outrunner or pancake motor. However, various combinations of these motor concepts are also possible. The illustration shows the combination of all three options (“around-runner”). The choice of a combination is based, among other things, on the proportions of the stator.

In addition, the field strength, scaling and shape of the magnets can be adapted to the requirements. There are also possibilities for variation in the number of pole pairs. In principle, the motor also works without alternate polarisation of the magnets, so that the number of pole pairs is no longer decisive, but simply the number of magnets. We originally tested such a “homopolar” version as well, but did not pursue it further.

- **Stator:**

The proportions of the stator and thus of the winding core range from an annulus in pancake models, through the illustrated toroid with a rectangular profile, to a thin-walled hollow cylinder, whereby the lateral magnets are no longer necessary.

As explained in section 3, the choice of the number of windings n and circulations m as well as the detailed geometry of the windings results in countless possibilities to vary the stator. The same applies to the choice of the winding wires used.

- **Construction:**

Depending on the requirements, it may be useful to position the winding mount on the side rather than axially centred. Furthermore, the bearings do not have to be mounted axially symmetrically.

- **Scaling:**

Electric machines are scalable. The RNT motor can also be designed in a wide range of sizes, depending on the power requirements.

3 The Toroidal Windings

The windings are based on the concept of a toroidal coil, where the wire is wound around a ring shaped core. The number of windings for one circulation around the ring is labelled as n . Figure 2 shows a toroidal coil with $n = 15$.

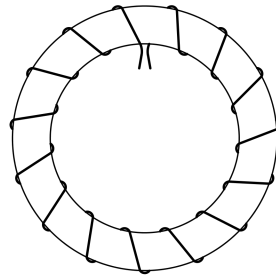


Fig. 2: A toroidal coil with $n = 15$ windings.

For the construction of the RNT motor, the core of the windings is made of a non-ferromagnetic, electrically insulating material. It is possible to realize the cooling of the windings by means of a heat exchanger placed inside the core.

The windings for one phase consist of a toroidal coil with n windings and m circulations. Figure 3a) shows the windings for one phase with $n = 15$ and $m = 5$, where the core with outer and inner diameter d_1 and d_2 has a rectangular profile with side lengths s_1 and s_2 . In principle, toroids with other profiles are also possible. The wire is tightly wound so that the windings of one phase cover one third of the core almost or completely. Depending on the number of windings n , several layers can be wound. The windings of the three phases are staggered and cover the core evenly.

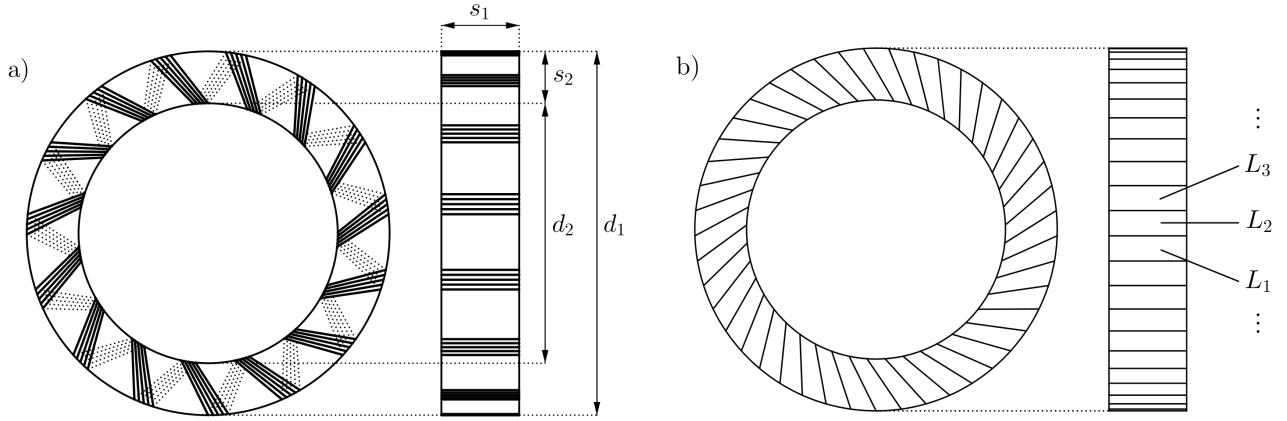


Fig. 3: a) Winding of one phase with $n = 15$ and $m = 5$.
The dotted lines in axial view (left) illustrate the wire on the back.
b) Three phases L_1 , L_2 und L_3 staggered.

For a current-carrying, ideally wound toroidal coil where the wire completely and evenly covers the core, the magnetic field outside the coil has mainly axial and radial components resulting from the circulation of the wire around the toroid. The magnetic field component in circumferential direction is limited to the inside of the ideal toroidal coil. The toroidal coil of a single phase, on the other hand, has gaps between the windings. Moreover, all three phases never carry the same current at the same time. Thus the live coil also has an optimally usable magnetic field component in circumferential direction outside.

In the example shown in figure 3, the pitch of the winding is applied exclusively laterally as it circulates around the toroid. The wire inside and outside, however, runs parallel to the toroid axis and therefore does not contribute to the pitch. Alternatively, the pitch can be shifted to other locations. For example, in a pure pancake model with $s_1 \ll s_2$, where the inner and outer magnets are omitted, the pitch can be applied inside and/or outside. If magnets are positioned above the inclined wires, it is advantageous to arrange the incline symmetrically (e.g. as in figure 3a on *both* sides of the toroid, or inside *and* outside). In this way, the mean radial or axial force components on the magnets, which do not contribute to rotation, compensate each other during operation. This circumstance will be discussed in more detail in section 5.

4 Magnets

The outer and inner magnets are attached to thin-walled hollow steel cylinders, the lateral magnets to annulus-shaped steel discs. In order to obtain the highest possible torque, up to n pole pairs can be attached.

Magnets over inclined wires are mounted at the same angle of inclination so that the longitudinal axis of a magnet centred over a phase is parallel to the central wires. Figure 4 illustrates the positioning of the magnets for 15 pole pairs for the windings from figure 3. On the left, the positioning of the magnets on the hollow cylinders relative to the stator is shown for a rotor position where one pole is centred over one of the phases. On the right, the positioning and polarisation of the lateral magnets is shown. The two lateral discs are identical. In the axial full section in the middle, the relative positioning of the hollow cylinders, the discs, and the stator is shown. The stator mount, the bearings, and the stator axis are shown as dashed lines. In the example shown, the stator mount is located in the middle between the lateral discs.

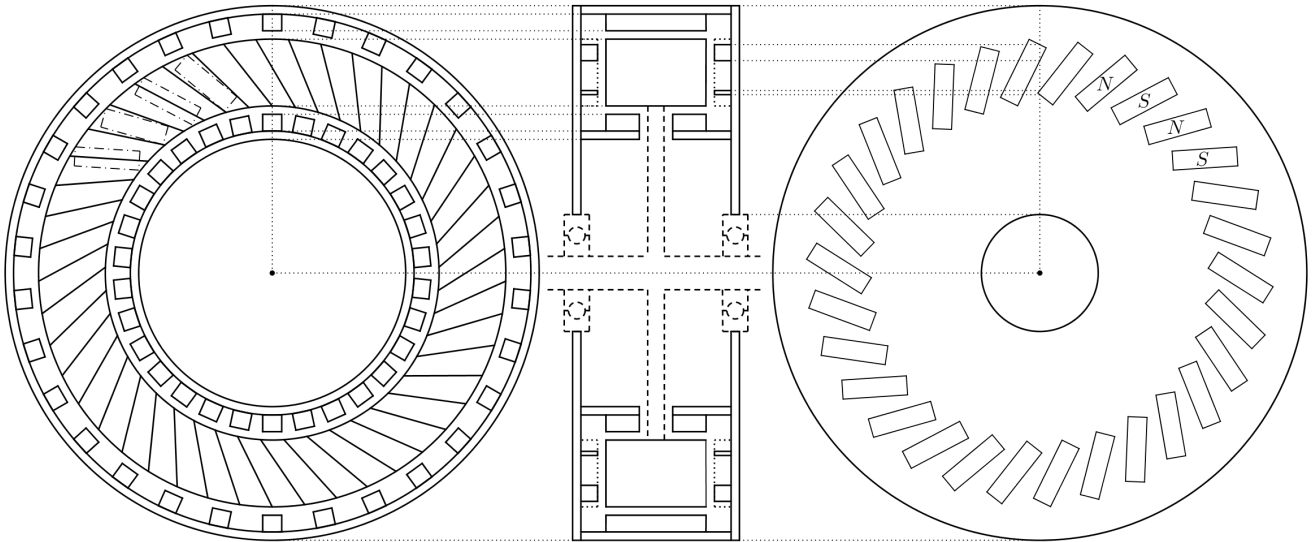


Fig. 4: *Left:* The outer and inner magnets are attached to thin-walled hollow steel cylinders.
Right: The lateral magnets are attached to annulus-shaped steel discs.
Middle: In the example shown, the rotor is made up of one outer and two inner hollow cylinders and two side discs. The stator mount, the bearings, and the stator axis are indicated by dashed lines.
To clarify the construction: The lateral discs are attached to the front and rear in relation to the view on the left. On the rear side, the disc is mounted as shown on the right. For the front, it is rotated 180° so that the magnets inscribed with poles are positioned above the dotted rectangles.

The polarisation of the magnets is chosen in such a way that above a phase the same pole is always facing the wire. Figure 5a shows the polarisation of the inner and outer magnets for a position of the rotor where the north pole is centred over one of the three phases. Figure 5b shows the corresponding positioning of the lateral magnets. The dotted lines show the situation on the rear side. The north pole of the magnets in bold is pointing towards the wire, corresponding to the situation in figure 5a.

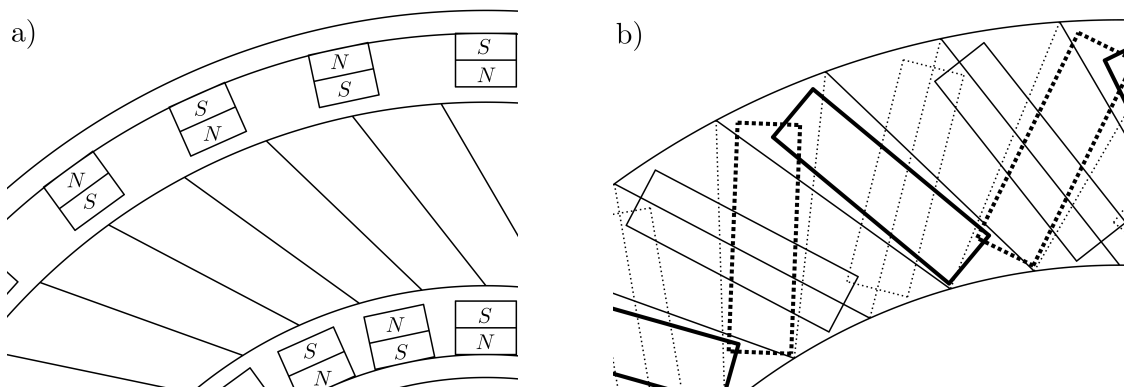


Fig. 5: Detailed view:
 a) Polarisation of the inner and outer magnets.
 b) Positioning of the lateral magnets. The north pole of the magnets in bold is pointing towards the wire. (Dotted: rear side)

5 Operating Principle

The operating principle of the motor can be explained very simply with the concept of Lorentz force. Figure 6 shows a cuboid magnet of length l as well as a piece of wire above the north pole. The magnetic flux density \vec{B} of the magnet points upwards from the north pole. For the sake of simplicity we assume that the distance between the wire and the magnet is sufficiently small so that the wire is in an approximately homogeneous \vec{B} field. If the wire carries the current I as shown in the diagram, it is subject to the Lorentz force directed to the right,

$$\vec{F}_L = l \cdot \vec{I} \times \vec{B},$$

where $\vec{a} \times \vec{b}$ is the cross product of two vectors \vec{a} and \vec{b} .

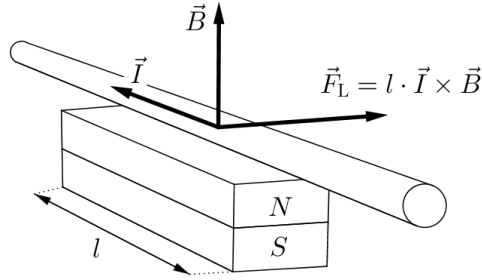


Fig. 6: A current-carrying piece of wire in the magnetic field of a magnet of length l . The current vector \vec{I} and the magnetic flux density \vec{B} of the magnet yield the Lorentz force $\vec{F}_L = l \cdot \vec{I} \times \vec{B}$.

According to Newton's third law, the magnet is subject to a force in the opposite direction to the left. In the motor the conductor is part of the stator and thus fixed, while the magnet as part of the rotor is movable and accelerates.

For the example shown in figures 3-5, \vec{F}_L is tangentially aligned for the inner and outer magnets, so that the full force is available for acceleration in the rotational direction. For the lateral magnets, however, \vec{F}_L has a radial component due to the angle of inclination. This is shown in figure 7.

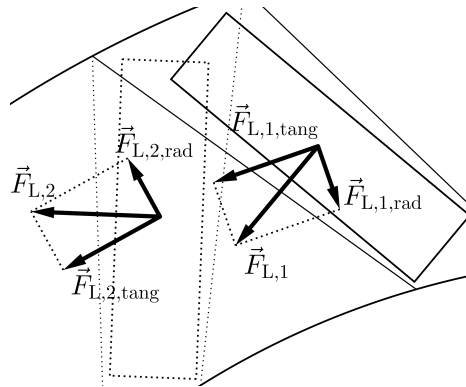


Fig. 7: For the example shown in figures 3-5, the Lorentz force on the lateral magnets has a tangential component $\vec{F}_{L,i,tang}$ as well as a radial component $\vec{F}_{L,i,rad}$, which does not contribute to the angular acceleration of the rotor.

Even if the mean radial force components compensate each other, they lead to undesired shears in the rotor. The same applies to axial force components, which can occur when the winding pitch is shifted from the sides to other places. These shears can be avoided by not positioning magnets over inclined wires. On the other hand, it is desirable to use the available winding wire as much as

possible for the generation of torque. If no magnets are positioned above the inclined wire sections, their length should be minimised. Otherwise, the pitch angle of the winding should be as small as possible.

6 Measurement Results from Prototypes

In this last section we compile some measurement series for three different prototypes. The measurements were carried out on a conventional motor test bench with a precision torque sensor. We used LiPo accumulators as power source. For each measurement series, the number of LiPo cells connected in series is given, each of which has a nominal voltage of 3,3 V or a voltage of 4,2 V when fully charged.

For each series of measurements, the voltage U , the current I , the torque M and the RPM z were measured with increasing load. The tables also show the instantaneous values calculated from these measurements for the input power

$$P_{\text{in}} = I \cdot U ,$$

the output power

$$P_{\text{out}} = \frac{\pi}{30} \cdot M \cdot z ,$$

and the efficiency

$$\eta = \frac{P_{\text{out}}}{P_{\text{in}}} .$$

We have omitted calculations for the error propagation of the measurement inaccuracies.

To illustrate the measurement series, we have prepared graphs showing the measured values for U , M and z as a function of I . For each of the three quantities U , M and z , the graphs of the quadratic (polynomial) regressions $\hat{U}(\hat{I})$, $\hat{M}(\hat{I})$ and $\hat{z}(\hat{I})$ were also plotted. The efficiency curve was calculated from the regressions, i.e.

$$\eta(\hat{I}) = \frac{\pi \cdot \hat{M}(\hat{I}) \cdot \hat{z}(\hat{I})}{30 \cdot \hat{U}(\hat{I}) \cdot \hat{I}} .$$

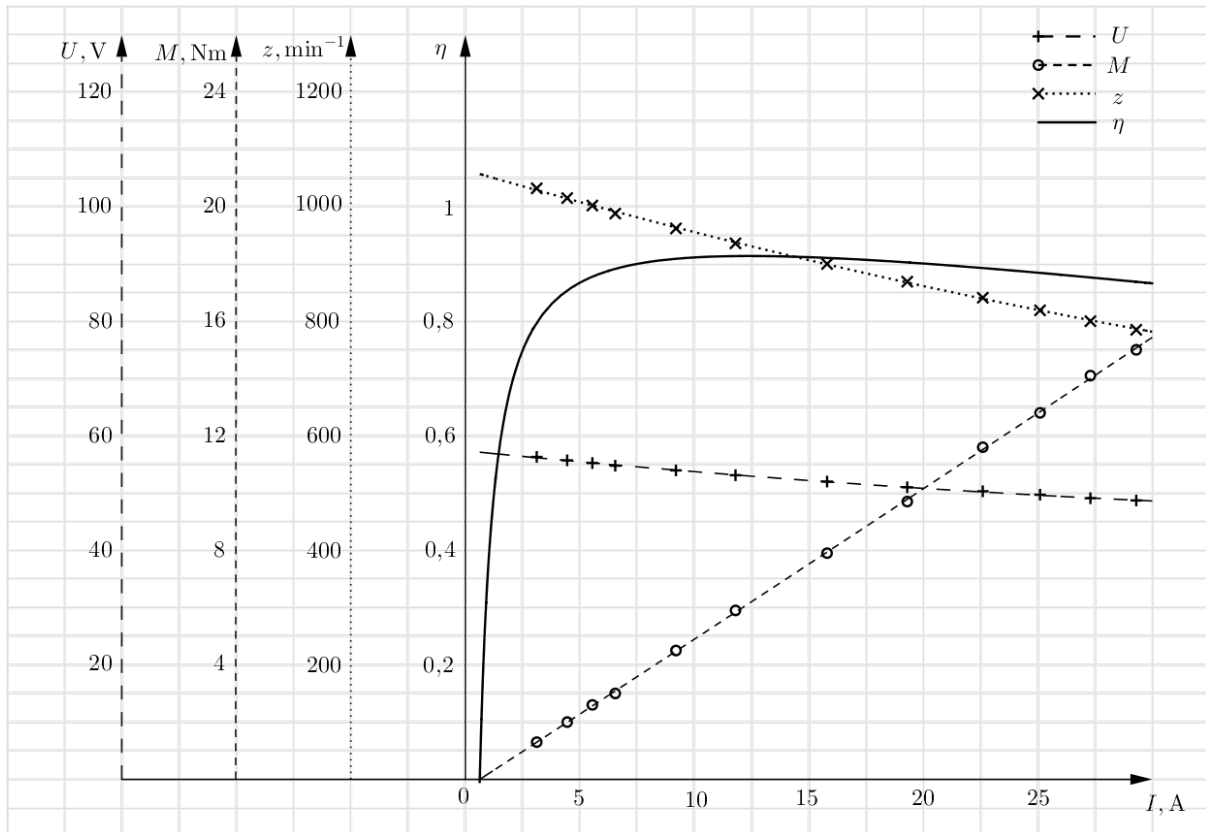
Optimisations can be used to bring the typical torque and RPM closer to values desired for a given application. On the one hand, the parameters can be adjusted as described in section 2. On the other hand, dissipation can be reduced by a more precise design and optimised bearing. It is quite conceivable that, with suitable optimisation, maximum efficiencies can be achieved which are higher than the values presented here.

Prototype 1:

This prototype was originally designed as a hub motor for an electric bicycle. However, the RPM is too high for this application, while the torque is rather too low.

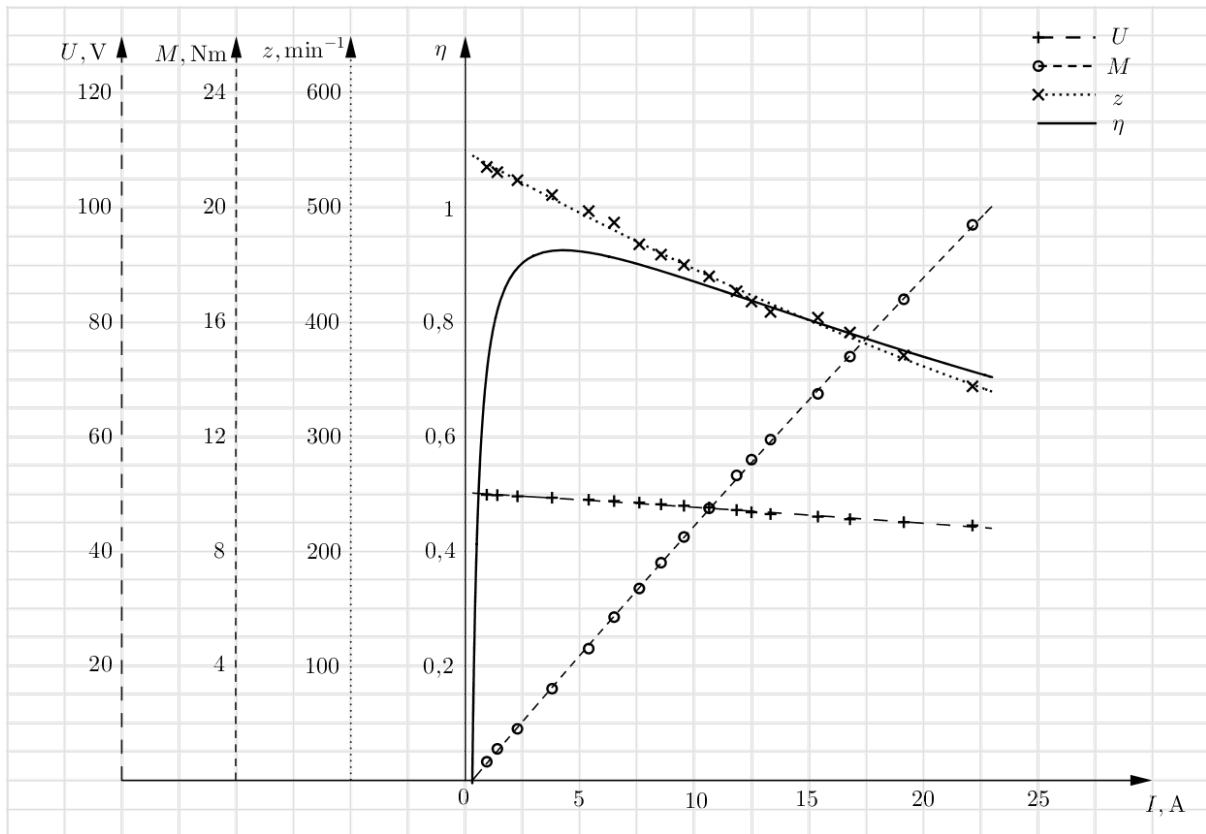
Delta connection with 14 LiPo cells in series ($K_V \approx 18,5 \frac{1}{\text{min V}}$):

U, V	I, A	P_{in}, W	M, Nm	$z, 1/min$	P_{out}, W	η
56.3	3.1	176	1.3	1032	140	0.80
55.7	4.5	248	2.0	1015	213	0.86
55.2	5.6	307	2.6	1002	273	0.89
54.8	6.6	359	3.0	988	310	0.87
54.0	9.2	496	4.5	962	453	0.91
53.1	11.8	627	5.9	936	578	0.92
52.0	15.8	822	7.9	900	745	0.91
51.0	19.3	984	9.7	869	883	0.90
50.3	22.6	1137	11.6	841	1022	0.90
49.7	25.1	1247	12.8	819	1098	0.88
49.1	27.3	1340	14.1	800	1181	0.88
48.7	29.3	1427	15.0	785	1233	0.86



Star connection with 12 LiPo cells in series ($K_V \approx 10,9 \frac{1}{\text{minV}}$):

U, V	I, A	P_{in}, W	M, Nm	$z, 1/min$	P_{out}, W	η
49.9	0.9	47	0.7	536	36	0.78
49.8	1.4	70	1.1	531	61	0.88
49.6	2.3	113	1.8	524	99	0.87
49.4	3.8	187	3.2	511	171	0.92
49.0	5.4	264	4.6	497	239	0.91
48.8	6.5	317	5.7	487	291	0.92
48.5	7.6	369	6.7	468	328	0.89
48.2	8.6	412	7.6	459	365	0.89
48.0	9.6	458	8.5	450	401	0.87
47.7	10.7	507	9.5	440	438	0.86
47.2	11.9	559	10.7	427	476	0.85
46.8	12.5	585	11.2	418	490	0.84
46.5	13.3	620	11.9	409	510	0.82
46.1	15.4	709	13.5	404	571	0.81
45.6	16.8	766	14.8	391	606	0.79
45.1	19.2	863	16.8	371	653	0.76
44.5	22.2	986	19.4	344	699	0.71

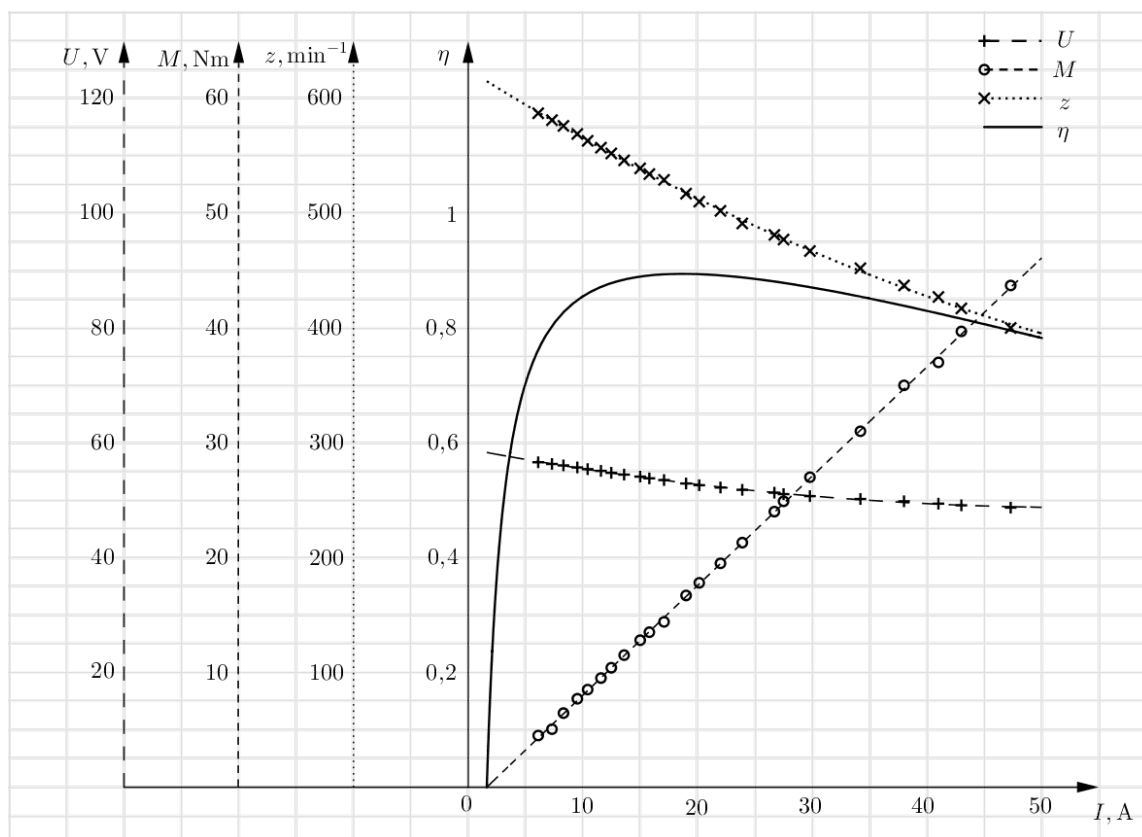


Prototype 2:

A rim motor for an electric bicycle. Both the RPM and the torque are close to the desired values for this application.

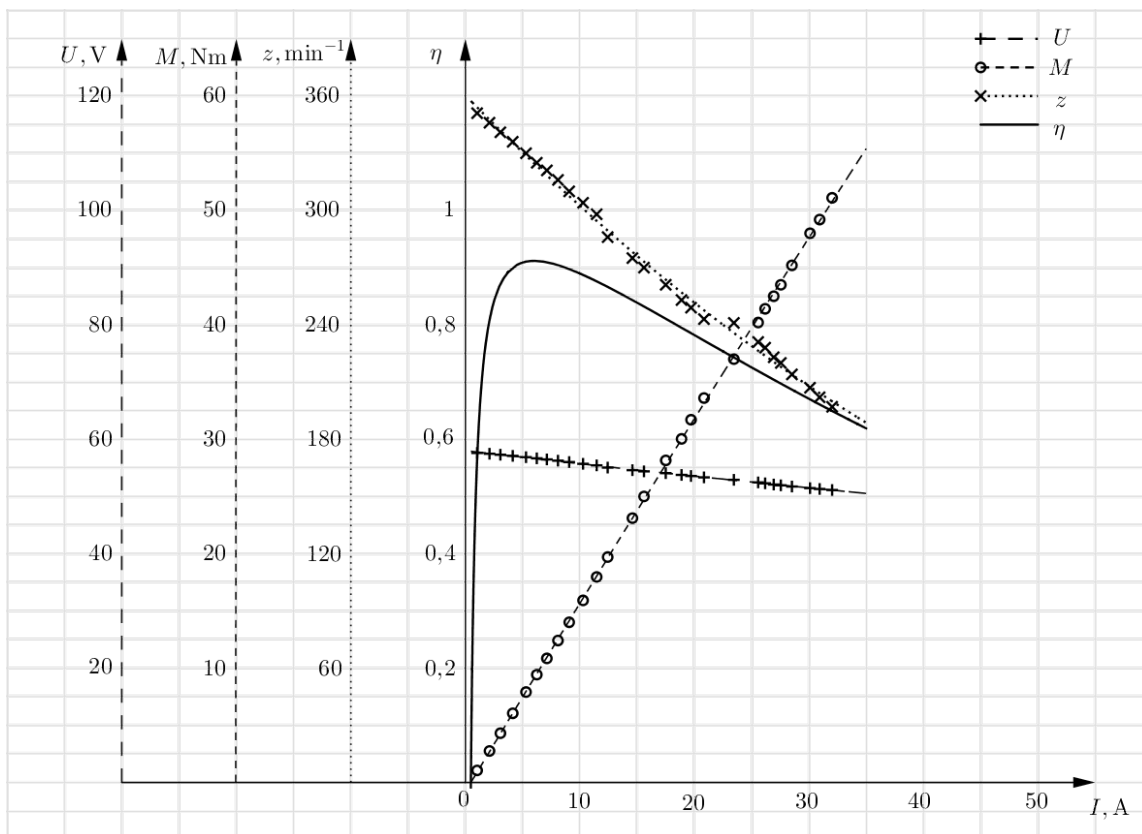
Delta connection with 14 LiPo cells in series ($K_V \approx 10,5 \frac{1}{\text{min V}}$):

U, V	I, A	P_{in}, W	M, Nm	$z, 1/min$	P_{out}, W	η
56.6	6.1	346	4.5	587	277	0.80
56.3	7.3	412	5.1	581	307	0.75
56.1	8.3	466	6.5	576	389	0.84
55.7	9.5	530	7.7	569	459	0.87
55.4	10.4	577	8.5	563	501	0.87
55.1	11.6	638	9.5	557	554	0.87
54.8	12.5	683	10.4	552	601	0.88
54.5	13.6	741	11.5	546	658	0.89
54.1	15.0	812	12.8	539	722	0.89
53.8	15.8	850	13.5	534	755	0.89
53.5	17.1	914	14.4	529	798	0.87
52.9	19.0	1005	16.7	517	904	0.90
52.6	20.2	1060	17.8	510	951	0.90
52.2	22.0	1148	19.5	502	1025	0.89
51.8	23.9	1238	21.3	491	1095	0.88
51.3	26.7	1370	24.0	481	1209	0.88
51.1	27.5	1404	24.9	477	1244	0.89
50.7	29.8	1511	27.0	467	1320	0.87
50.2	34.2	1717	31.0	452	1467	0.85
49.8	38.0	1892	35.0	437	1602	0.85
49.4	41.0	2025	37.0	427	1654	0.82
49.1	43.0	2111	39.7	417	1734	0.82
48.7	47.3	2304	43.7	400	1831	0.79



Star connection with 14 LiPo cells in series ($K_V \approx 6,2 \frac{1}{\text{minV}}$):

U, V	I, A	P_{in}, W	M, Nm	$z, 1/min$	P_{out}, W	η
57.6	1.0	59	1.1	351	39	0.65
57.5	2.1	121	2.8	346	100	0.82
57.3	3.1	175	4.3	341	154	0.88
57.1	4.1	236	6.0	336	213	0.90
56.9	5.3	301	7.9	330	273	0.91
56.7	6.2	354	9.4	325	321	0.91
56.5	7.1	402	10.8	321	364	0.91
56.3	8.1	455	12.4	316	410	0.90
56.0	9.1	508	14.0	310	454	0.89
55.7	10.3	573	15.9	304	506	0.88
55.4	11.5	636	18.0	298	560	0.88
55.0	12.4	684	19.7	286	590	0.86
54.6	14.6	796	23.1	275	665	0.84
54.4	15.6	848	25.0	270	707	0.83
54.1	17.5	946	28.2	261	769	0.81
53.8	18.9	1015	30.0	253	796	0.78
53.6	19.7	1056	31.7	249	827	0.78
53.3	20.8	1111	33.6	243	855	0.77
52.9	23.5	1241	37.0	241	934	0.75
52.5	25.6	1341	40.2	231	972	0.73
52.3	26.2	1369	41.4	228	988	0.72
52.1	26.9	1403	42.5	223	992	0.71
51.9	27.6	1431	43.5	220	1002	0.70
51.7	28.5	1475	45.2	214	1013	0.69
51.5	30.1	1549	48.0	207	1040	0.67
51.3	30.9	1587	49.2	202	1041	0.66
51.1	32.0	1637	51.1	197	1054	0.64

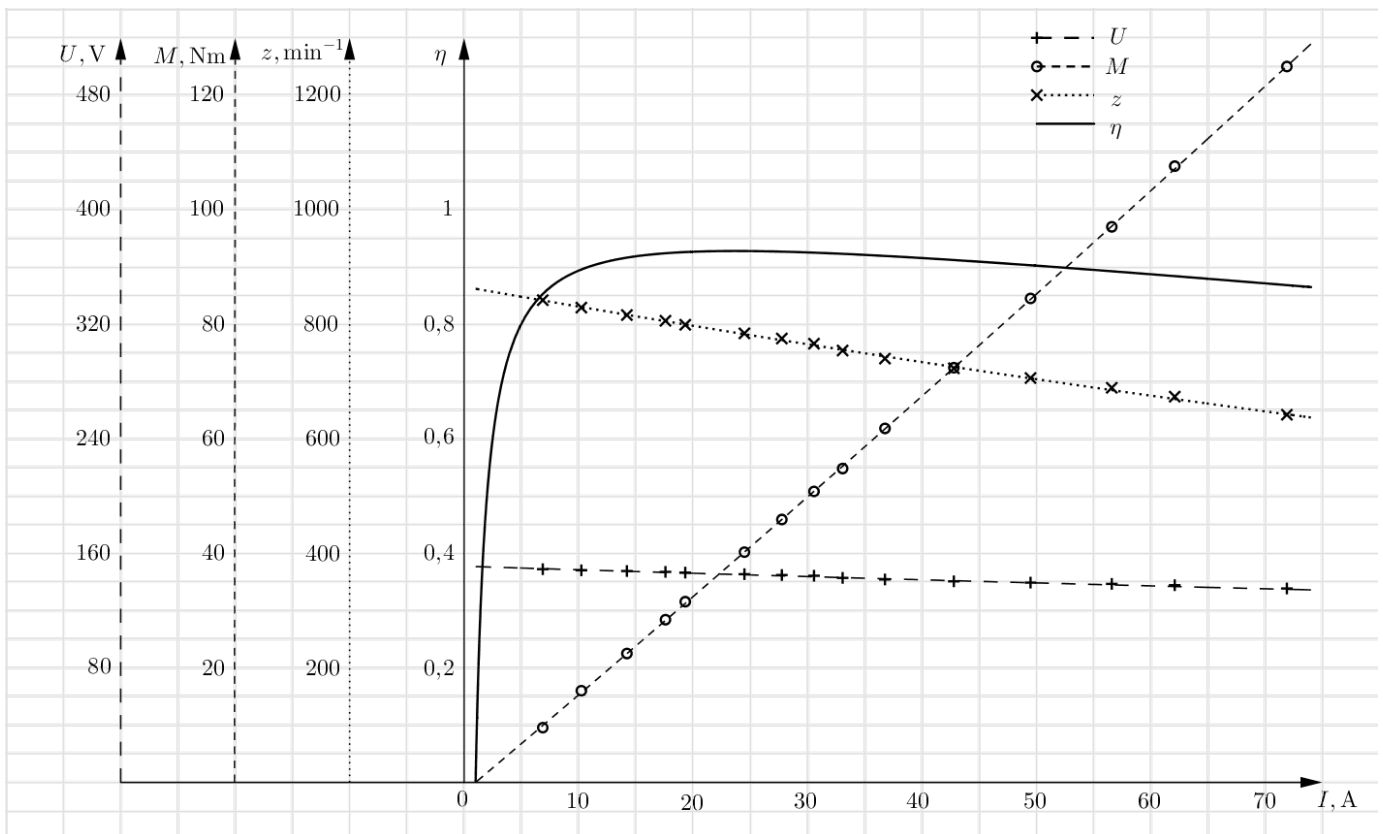


Prototyp 3:

This prototype was designed as a rim motor for light weight vehicles. For an application in four-wheeled vehicles, two or four wheels would be equipped with one motor each. If necessary, propulsion can also be carried out using an axle gear.

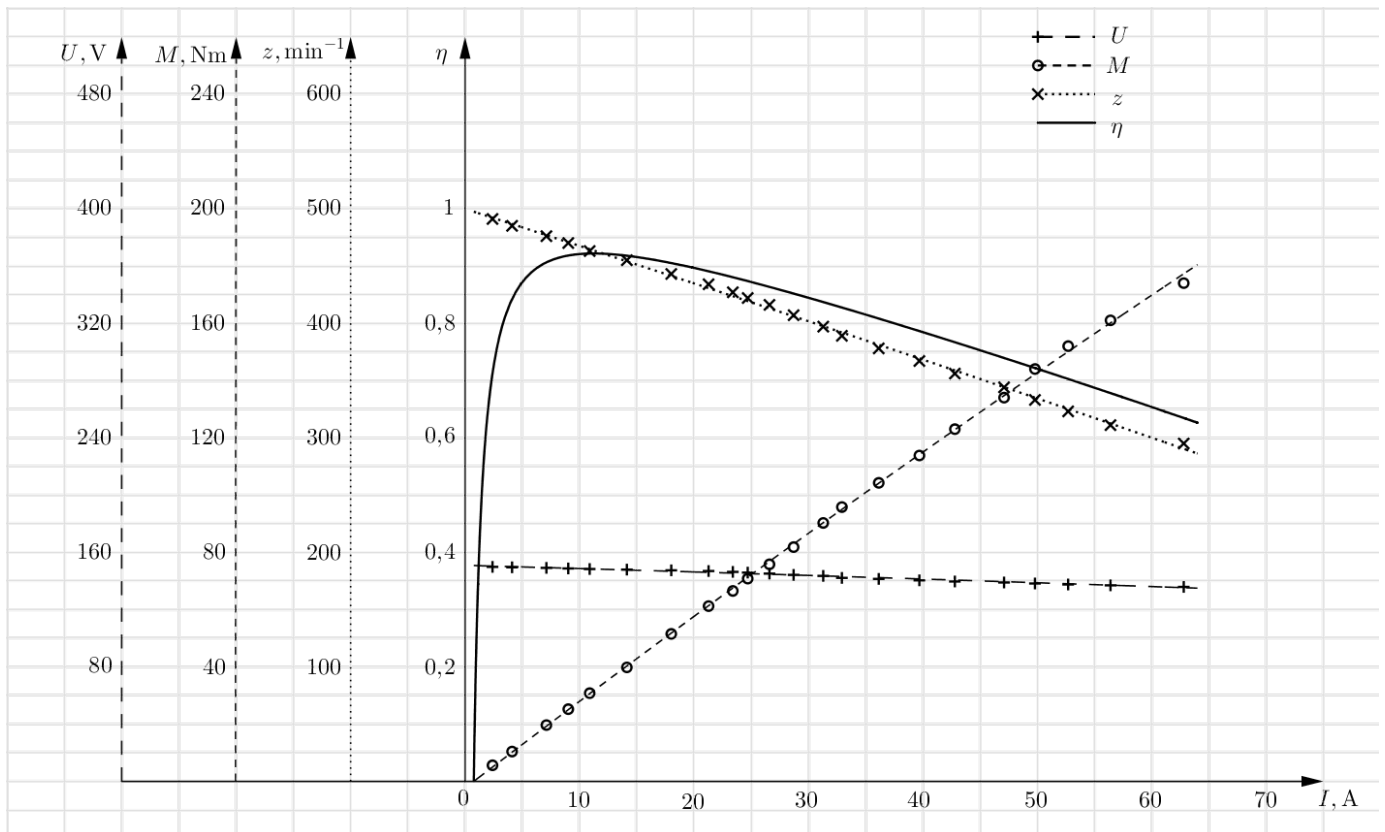
Delta connection with 36 LiPo cells in series ($K_V \approx 5,7 \frac{1}{\text{min V}}$):

U, V	I, A	P_{in}, kW	M, Nm	$z, 1/min$	P_{out}, kW	η
149	6.9	1.02	9.6	842	0.84	0.82
148	10.3	1.52	16.0	829	1.39	0.92
148	14.2	2.10	22.5	816	1.92	0.92
147	17.6	2.59	28.4	806	2.40	0.93
147	19.3	2.83	31.6	799	2.64	0.93
145	24.5	3.56	40.2	784	3.30	0.93
145	27.8	4.02	45.9	775	3.73	0.93
144	30.6	4.41	50.8	766	4.07	0.92
143	33.1	4.72	54.8	754	4.33	0.92
142	36.8	5.21	61.8	740	4.79	0.92
140	42.8	6.01	72.4	723	5.48	0.91
140	49.5	6.91	84.5	706	6.25	0.90
139	56.6	7.84	97.0	689	7.00	0.89
138	62.1	8.55	108	674	7.59	0.89
135	71.9	9.74	125	642	8.40	0.86



Star connection with 36 LiPo cells in series ($K_V \approx 3,3 \frac{1}{\text{minV}}$):

U, V	I, A	P_{in}, kW	M, Nm	$z, 1/min$	P_{out}, kW	η
150	2.4	0.36	5.6	491	0.29	0.80
150	4.1	0.61	10.4	485	0.53	0.86
149	7.1	1.06	19.7	476	0.98	0.92
149	9.0	1.34	25.2	470	1.24	0.92
148	10.9	1.61	30.8	463	1.49	0.92
148	14.1	2.09	39.8	455	1.90	0.91
147	18.0	2.66	51.5	443	2.39	0.90
147	21.3	3.13	61.2	434	2.78	0.89
146	23.4	3.42	66.5	427	2.97	0.87
146	24.7	3.60	70.8	422	3.13	0.87
145	26.6	3.86	75.8	416	3.30	0.86
144	28.7	4.14	81.8	407	3.49	0.84
144	31.3	4.49	90.3	397	3.75	0.84
142	32.9	4.68	95.8	389	3.90	0.83
141	36.2	5.11	104	378	4.13	0.81
140	39.7	5.57	114	367	4.37	0.78
140	42.8	5.97	123	356	4.59	0.77
139	47.1	6.54	134	344	4.83	0.74
138	49.8	6.88	144	333	5.02	0.73
138	52.7	7.25	152	323	5.14	0.71
137	56.4	7.72	161	311	5.24	0.68
136	62.8	8.53	174	295	5.38	0.63



Delta connection with 84 LiPo cells in series ($K_V \approx 5,7 \frac{1}{\text{min V}}$):

U, V	I, A	P_{in}, kW	M, Nm	$z, 1/min$	P_{out}, kW	η
343	22.5	7.7	35.5	1889	7.0	0.91
340	36.4	12.4	60.0	1832	11.5	0.93
335	49.5	16.6	85.0	1774	15.8	0.95
327	54.9	17.9	93.5	1709	16.7	0.93
324	58.6	19.0	101	1685	17.8	0.94
322	61.4	19.8	106	1667	18.5	0.94
320	64.1	20.5	111	1651	19.1	0.93
318	70.9	22.5	124	1618	21.0	0.93

